Nadere info:

Thank you for contacting Nature Research about the self-archiving policy for Nature Research journals.

Authors publishing in *Nature* and in all other Nature Research journals are able to make the accepted version of their manuscript openly available six months after publication through self-archiving in the repository of their choice (see the full details of our self-archiving policy). Please note that the version which may be archived is the manuscript accepted following peer-review and author revision, but prior to copyediting and typesetting by Nature Research.

We also offer a free Nature Research Manuscript Deposition Service to all original research articles published in *Nature*, the Nature Research journals, and many of our society and academic journals. Corresponding authors whose funders have agreements with PubMed Central, Europe PubMed Central, and PubMed Central Canada may opt in to this service during submission. Nature Research will archive the accepted version of the manuscript on behalf of the author, and it will be made publicly accessible six months after publication with links back to the journal's website. For further information, please see here.

Responsive Biomimetic Cytoskeletal Networks from Polyisocyanopeptides Hydrogels

Paul H.J. Kouwer[1†]*, Matthieu Koepf[1†], Vincent A.A. Le Sage[1], Maarten Jaspers,[1] Arend M. van Buul[1], Zaskia Eksteen[1], Tim Woltinge[1], Erik Schwartz[1], Heather J. Kitto[1], Richard Hoogenboom[1,3], Stephen J. Picken[2], Roeland J.M. Nolte[1], Eduardo Mendes[2], and Alan E. Rowan[1]*.

Author affiliations

[1] Radboud University Nijmegen, Institute for Molecules and Materials, Department of Molecular Materials, Heyendaalseweg 135, 6525 AJ Nijmegen, The Netherlands.

[2] Delft University of Technology, Department of NanoStructured Materials, Julianalaan 136, 2628 BL Delft, The Netherlands.

[3] Current address: Supramolecular chemistry group, Department of Organic Chemistry, Ghent University, Krijgslaan 281-S4, 9000 Ghent, Belgium.

[†] These authors contributed equally to this work.

* Correspondence to: a.rowan@science.ru.nl, p.kouwer@science.ru.nl

Abstract

Responsive hydrogels applied in the biomedical area show great potential as synthetic extracellular matrix mimics and as host medium for cell growth. The hydrogels often lack the characteristic mechanical properties that are typically seen for natural gels. Here, we demonstrate the unique responsive and mechanical properties of hydrogels based on oligo(ethylene glycol) functionalized polyisocyanopeptides. These stiff helical polymers form gels upon warming at concentrations as low as 0.006 %-wt polymer, with materials properties almost identical to those of their intermediate filaments, a class of cytoskeletal proteins. Using a combination of macroscopic rheology and molecular force microscopy the hierarchical relationship between the macroscopic behaviour of theses peptide mimics has been correlated with the molecular parameters.

Material scientists often look to the natural world for both inspiration and instruction on how to develop responsive materials. Mechanical responsiveness is essential to all biological systems down to the level of tissues and cells. Tissues are responsive to deformation, can generate force and, in turn, force can affect cell and tissue formation. Cell mechanics are governed by the cytoskeleton, composed of stiff microtubules, actin filaments and intermediate filaments. The latter constitute family of fibrous α-helical proteins, which, at the appropriate aqueous conditions, self-assemble into semiflexible bundles with diameters (d_B) around 10 nm and typical persistence lengths (l_p) around 1 μm[1].

Recently, detailed theoretical and experimental studies on cytoskeletal materials have elucidated the strongly nonlinear mechanical properties of gels of these biological fibres[2], and have helped to highlight the fundamental parameters which control the mechanical response of entire cells[3]. A simple examination of these biomaterials yields an often recurring design motif: a high l_p, correlated strongly to the helical architecture of the individual fibrils and the bundles they form. As far as we know, there are no synthetic equivalents to these biogels that show similar mechanical behaviour. Here, we present a hydrogel with mechanical properties that nearly completely overlap with those of IFs and, moreover, by using appropriate network theories, we explain its hierarchical assembly behaviour at different length scales.

The material is based on synthetic polyisocyanopeptides (PICs)[4], which possess a 4_1 (four repeat units per turn) β-helical architecture, in which a hydrogen bond network has developed between the peptidic side groups parallel to the polymer backbone[5], resulting in exceptionally stiff chains; some polymers are amongst the stiffest manmade materials known to date with an l_p up to 200 nm[6]. This precise architectural definition has been utilised in their application in electronic applications[7]. We found that a family of water-soluble thermoresponsive oligo(ethylene glycol) functionalized PICs is able to gel water with an extraordinary high efficiency[8-10]. Such hydrogel materials are very attractive in, for instance, the fields of drug delivery[11], regenerative surgery[12] and advanced stimuli-responsive systems[13,14].

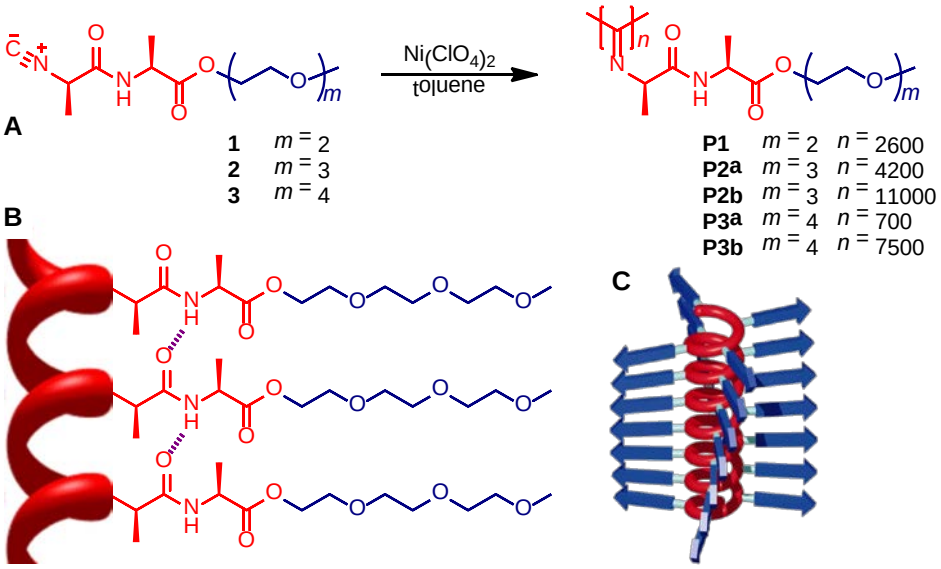

Figure 1 | Oligo(ethylene glycol) substituted polyisocyanopeptides. a, Synthesis of the polymers – the degree of polymerisation is estimated from AFM experiments. **b,** Representation of the hydrogen-bond network that stabilises the secondary helical structure for **P2**. **c,** Schematic illustration of the 4_1 β-sheet helix. The arrow represents the peptide substituents.

The hydrogels are composed of oligo(ethylene glycol) functionalised polyisocyanopeptides **P1-P3**. These polymers were obtained through a nickel(II)-catalysed polymerization of di-, tri-, and tetraethylene glycol functionalized isocyano-(*D*)-alanyl-(*L*)-alanines **1-3** (Fig. 1) using a previously described procedure.[15] Variation of the catalyst to monomer ratio allowed us to tune the molecular weights of the polymers, which were determined by atomic force microscopy (AFM) experiments (see Supplementary). The hydrogen-bonded 4_1 helical structure of the polymer backbone was confirmed by infrared (IR) and circular dichroism (CD, Supplementary Fig. S1) spectroscopies. In aqueous solution and in the gel phase the secondary structure of the polymer is stable up to 70 °C as shown with CD experiments (Figs. S2, S3). The combination of the densely-packed helical structure and the strong intramolecular hydrogen-bonded network gives rise to stiff polymer chains[6], which could be readily visualized with AFM after drop casting or spin coating from a dilute solution onto mica (Fig. 2a and Fig. S4).

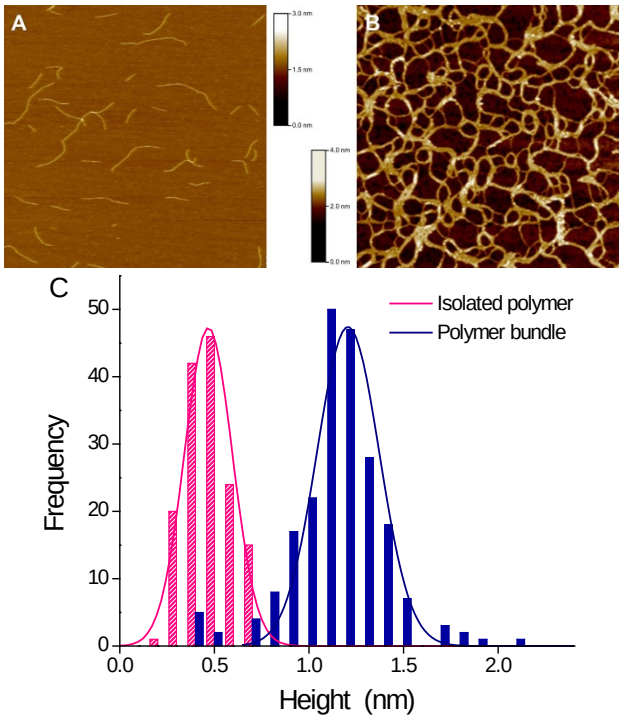

Figure 2 | AFM analysis of polymers and gel. a, AFM image of isolated polymer chains of **P2b**. **b,** AFM image of bundles of **P2b** from gels. **c,** Statistical height histograms of both isolated chains and bundles. Both show similarly narrow distributions: chain height h_0 = 0.46 ± 0.13 nm and bundle diameter h_B = 1.21 ± 0.16 nm.

Thermal analysis of dilute aqueous solutions of **P2b** and **P3b** showed the formation of transparent hydrogels upon heating at 18 and 44 ºC, respectively[16]. The sol-gel phase transition was

very fast (seconds time scale) fully reversible and thermal cycles between 0 and 70 ºC did not noticeably shift the transition temperatures. The structure of the gel was visualised by AFM (Fig. 2b and Fig. S5a-e) and cryoSEM (Fig. S5f). Both techniques showed the formation of a network, composed of strands, typically built-up from bundles of polymer chains, where occasionally single polymer chains could be observed as well. The extent of bundling was estimated by statistical analysis of the AFM images of the bundles and the isolated polymer chains (Figure 2C). The narrow distributions of relative heights was used to abstract the bundle number (average number of polymer chains per bundle) N = 6.9, using the relation $N = d_B^2/d_0^2 \approx h_B^2/h_0^2$, where d_0 and d_B are the diameters and h_0 and h_B the heights of isolated chains and a bundles[17]. Interestingly, we found that the bundle dimensions were constant irrespective of the concentration. AFM analysis of the gels obtained at high concentrations showed a strong increase in the number of bundles, but not in the bundle dimensions (Fig. S6). Preliminary single particle tracking studies of gels of **P2b** show nanoparticle diffusion coefficients that strongly scale with concentration (Fig S7). This confirms that at higher concentrations more bundles, (and hence smaller pores which results in restricted particle displacement) rather than thicker bundles are formed. This self-limiting behaviour of bundle formation is thought to be related to the chirality (i.e. the helical pitch) and the intrinsic stiffness of the polymer molecules[18]. As a consequence of a fixed bundle size the average pore size in the gel is directly controlled by the polymer concentration. Chain bundling is commonly observed for cytoskeletal polymers and the bundle properties (dimensions, stiffness) are critical parameters in the mechanical properties of those gels. For gels based on actin or IFs, bundling is controlled by additives, ranging from binding proteins[19] to divalent metal ions[20], whilst bundle formation in the polyisocyanopeptides gels is thermally activated.

The process of thermally induced gel formation is attributed to hydrophobic effects caused by the ethylene glycol tails grafted to the polyisocyanide backbone. Flexible oligo(ethyleneglycol) grafted polymers have been reported to show sharp order-disorder transitions at the lower critical solution temperature (LCST)[21]. Previous studies have demonstrated a linear relationship between the transition temperature and the average length of ethyleneglycol tail over a broad temperature range[22]. Upon heating **P2** and **P3**, the entropic desolvation of the ethyleneglycol arms gives rise to more hydrophobic chains that separate from the aqueous solution. Indeed, low molar mass polymers **P2a** and **P3a** precipitate at the transition temperature, in line with what has been observed for flexible (co)polymers. Longer polymers, however, yield completely transparent gels at the LCST, as the long chains are kinetically trapped in a network structure before they precipitate. Even at very low concentrations, gels are able to support their own weight during vial inversion tests. A sample of **P2b** passed the inversion test at a concentration as low as 0.006 wt-%, (Fig. S8) which is about an order of magnitude lower in concentration than many of the well-known synthetic superhydrogelators[23].

To learn more about their mechanical properties, the polymer gels were subjected to a full variable temperature rheological analysis. Samples were measured in a Couette configuration with small oscillatory deformations at different frequencies and amplitudes in the linear response regime (Figs. S9 and S10). A broad range frequency sweep in the gel phase (Fig. S10) corroborates that the crosslinks formed at the LCST are permanent in nature. Temperature sweeps of **P2b** and **P3b** (Figs. 3a, S11) show at low temperatures liquid-like behaviour with a storage modulus G' lower than the loss modulus G''. A sharp transition, at a temperature dependent on the length of the ethylene glycol

tail, marks gel formation and the moduli reach a plateau value G_0. The sol-gel transition temperature, rheologically determined as the onset of the step in G' at frequency ω = 6.2 rad s^{-1} (f = 1 Hz, Supplementary Fig. S12), shows little dependence on the polymer concentration c. The absolute value of G_0, however, is strongly correlated to c. Analysis showed a power law behaviour, $G_0 \propto c^n$ with coefficients n of 2.2 and 2.7 for **P2b** and **P3b**, respectively. These experimental values are in line with the theory of permanently linked semi-flexible networks that display purely entropic elasticity[24] (where n = 11/5), with other experimental studies based on cross-linked cytoskeletal materials actin[25] and IF gels[2] (with $n = 2 - 2.5$), and also with other stiff materials such as DNA gels (n = 2.3)[26].

The resemblance in fibre dimensions and mechanical properties to IFs and the availability of IF network models prompted us to also examine the rheological behaviour of the polyisocyanopeptide gels in the nonlinear response regime. Unlike many synthetic polymers, the cytoskeletal proteins (IFs and actin) and other stiff biopolymers show a strong, and well-defined, nonlinear stress response after a critical stress σ_c is applied to the gels[27]. Although the origins of the effect are currently under debate[27-29], experimentally, the effect is well-described[2,24,27]. A small increase in the strain γ in this regime results in very high stress levels and often results in the rupture of the gel. To probe this regime carefully, we used the recently benchmarked pre-stress protocol[30] and determined the differential modulus K, defined as $K' = d\sigma/d\gamma$, as a function of applied stress (Fig. 3B). When scaled to G_0 and σ_c (Fig. 3C) all curves of **P2b** at different concentrations and temperatures reduce to a single master curve. Even in this nonlinear regime, our hydrogels remarkably resemble the physically or chemically cross-linked protein-based materials, by precisely displaying the theoretically predicted $K' \propto \sigma^{3/2}$ dependency[2].

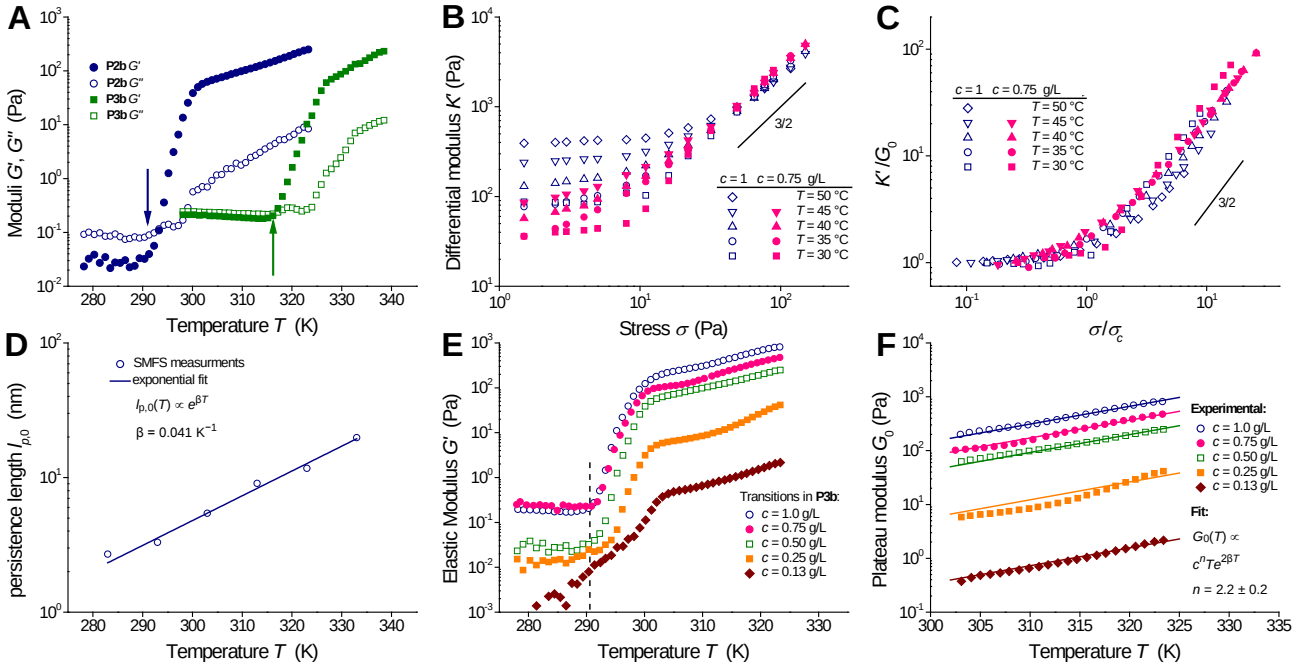

Figure 3 | Rheological analysis of polyisocyanopeptide gels. a, Moduli G' and G'' as a function of temperature T for **P2b** and **P3b** at c = 1.0 mg mL^{-1}. The arrows indicate the onset of the transition. **b,** Differential modulus K' as a function of stress σ. **c,** Data scaled with the plateau modulus G_0 and the critical stress σ_c. **d,** Single chain persistence length $l_{p,0}$ as a function of T of **P2b** between 10 and 60 °C measured by

SMFS. **e,** G' as a function of T for **P2b** at different concentrations. The dashed line at T = 18 °C shows that the onset of the gel temperature is nearly concentration independent, **f.** G_0 as a function of T and exponential fits to a single exponent β.

A theoretical model for semi-flexible networks, based on the extensible worm-like chain model[31], has been developed to explain the mechanical behaviour of actin[24] and IF-based hydrogels[2]. This model considers the network as a collection of thermally fluctuating bundles with length l_c as the average length between the crosslinks. Not only does it describe our experimental results accurately (*32*), it also yields information about the critical microscopic parameters, such as the persistence length of the bundles $l_{p,B}$ and l_c by applying eqs. 1 and 2 to the experimentally determined macroscopic quantities G_0 and σ_c:

$$G_0 = 6\chi \frac{c}{N} RT \frac{l_{p,B}^2}{l_c^3} \quad (1)$$

$$\sigma_c = \chi \frac{c}{N} RT \frac{l_{p,B}}{l_c^2}. \quad (2)$$

Here, χ combines molecular constants, c is the polymer concentration, N is the bundle number, R is the gas constant and T is the absolute temperature. Eqs. 1 and 2 show that G_0 and σ_c are dependent on N, $l_{p,B}$ and l_c, (which in turn also depends on concentration). Rheological measurements in the linear and in the nonlinear regime with c and T as experimental variables in combination with variable temperature Single Molecule Force Spectroscopy (SMFS) measurements allowed us to calculate $l_{p,B}$ and l_c. Unlike many other reports on hydrogels, these parameters have been verified independently.

SMFM measurements[6] provide information on the persistence length *of the individual polymer chains* $l_{p,0}$. In these experiments we determined force-distance curves of dilute polymer samples and subjected the results to the same extensible worm-like chain model that was applied to analyse the rheological data. Subsequent statistical analysis of the experimental data provided both the average for $l_{p,0}$, as well as its distribution (Fig. S14). SMFS measurements on **P2b**, equilibrated in water, typically yielded modest values for $l_{p,0}$ of the order of nanometres which is attributed to water decreasing the strength of the hydrogen bond network along the polymer backbone (see Supplementary). Interestingly, a temperature sweep between 10 and 60 °C, showed an exponential increase of the persistence length $l_{p,0}(T) \propto e^{\beta T}$ with an exponent β of 0.041 K^{-1} (Fig. 3d).

Figure 3e shows the plateau modulus $G_0(T)$ of **P2b** as a function of concentration and temperature as obtained by bulk rheological temperature sweeps. In the experimentally accessible window in the gel phase (30 °C > T > 50 °C) the plateau moduli at different concentrations showed an exponential increase in with T (Figure 3F). For this temperature range, the experimental results were successfully fitted to $G_0(T) \propto Te^{2\beta T}$, which also includes the theoretical linear thermal contribution of RT to the network stiffness. A fit to a single exponent $2\beta = 0.073$ K^{-1} describes the data at all concentrations surprisingly well. The only parameter in eq. 1 that depends on T is $l_{p,B}^2$. The fact that for single molecule measurements an exponent $\beta = 0.041$ K^{-1} was found, clearly indicates that the thermally induced increase in G_0 is simply the result of stiffening of the individual polymer

chains. This was confirmed by independent measurements of the critical stress σ_c as a function of temperature, which, at different concentrations, yielded a similar exponential behaviour with a value of $\beta = 0.049\ K^{-1}$, using eq. 2.

Combining eqs. 1 and 2 returns $l_{p,B}$ as a function of N, G_0 and σ_c; the last two experimentally determined by bulk rheology in the linear and nonlinear regime. By taking the bundle number $N \approx 7$ as estimated from the AFM measurements, a value of $l_{p,B}$ of of the order of hundreds of nanometer for **P2b** (1 mg mL^{-1}, 30 °C) was found, about two orders of magnitude larger than $l_{p,0}$. This can only be rationalised by considering that the bundles are strongly interacting, and behave effectively as a single fibre with the constituent strands 'glued' together. This so-called tight bundle regime is characterised by a square dependence of $l_{p,B}$ with N: $l_{p,B} = l_{p,0} N^2$; this is in contrast to the loose bundle regime, which shows a linear relationship[33]. Cross-linked biofibres, such as actin, show a transition from the tight to the loose bundle regime with increasing N. In line with these results, we also find a square dependency with for low bundle numbers. By establishing in which regime the bundles interact, we now can calculate N by straightforward comparison of the SMFS results and the (nonlinear) rheology data. Under the standard conditions (1 mg mL^{-1}, 30 °C), we find $N = 9.1$, which closely agrees with the value estimated from the AFM measurements. Calculations of N at different temperatures and concentrations yield very consistent numbers, further highlighting that for our materials, the bundle characteristics are intrinsic polymer properties, related to the secondary structure of the chains.

After determination of N, eqs. 1 and 2 provide the other unknown quantities: $l_{p,B}$ = 460 nm and l_c = 110 nm at c = 1 mg mL^{-1} and T = 30 °C; the latter is significantly smaller than $l_{p,B}$ as would be expected for a semi-flexible network. For fairly flexible bundles, a good approximation for l_c (that scales with c as $l_c \propto c^{-0.4}$) is the mesh size ξ (that scales as $\xi \propto c^{-0.5}$, see Supplementary Material). From the above results, a mesh size ξ = 140 nm was calculated.

Table 1 | Comparison of structural and mechanical properties between hydrogels based on polyisocyanide **P2b** and neurofilaments at similar concentrations.[2]

Characteristic gel property	**P2b**	**Neurofilaments**
bundle diameter d_B	7.5 nm[a]	10 nm
bundle number N	9	4
persistence length $l_{p,B}$ (1 mg mL^{-1})	460 nm	600 nm
deformation regime ($G_0 \propto c^n$)	entropic ($G_0 \propto c^{2.2}$)	entropic ($G_0 \propto c^{2.5}$)
G_0 (mg mL^{-1})	100 – 1000 Pa[b]	2 – 20 Pa[c]
high strain regime	strain stiffening ($K' \propto \sigma^{3/2}$)	strain stiffening ($K' \propto \sigma^{3/2}$)
contour length l_c (1 mg mL^{-1})	110 nm	300 nm

[a] Calculated based on N and an estimated cross section of the polymers; [b] temperature range: 30 °C < T < 60 °C; [c] Mg^{2+} concentration range: 2 mM < [Mg^{2+}] < 20 mM.

The model has now been modified to write G_0 and σ_c at given experimental conditions as a function of the intrinsic (temperature dependent) single chain persistence length, the bundle number and the length between crosslinks (see Supplementary):

$$G_0(T) \propto N^3 \frac{c}{l_c^3} RT l_{p,0}^2(T) \tag{3}$$

and

$$\sigma_c(T) \propto N \frac{c}{l_c^2} RT l_{p,0}(T) \tag{4}$$

Using eqs. 3 and 4 as a starting point, we can now speculate how these hydrogels can be further engineered. For instance, is it possible to go even lower in concentration, can we set the pore size of a hydrogel, or can we generate stiffer gels that mimic the properties of the other cytoplasmic materials.

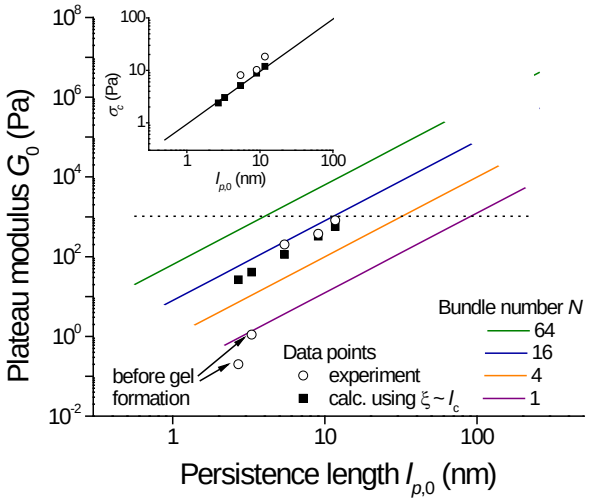

Figure 4 | Stiffness of the gel vs stiffness of a polymer. Calculated G_0 of **P2b** as a function of $l_{p,0}$ and N at c = 1 mg mL^{-1} from eq. 3 by substituting l_c for ξ with the experimental data (○) of **P2b** (c = 1 mg mL^{-1}) and the corresponding calculated data (■) using N = 9.1, at different temperatures. The dotted line at G_0 = 1 kPa is a guide to the eye. The inset shows the calculated σ_c with $l_{p,0}$, (eq. 4), which is independent of N as well as the calculated (■) and experimental (○) data points at T = 30, 40 and 50 °C.

To this end, we approximated the experimentally poorly accessible length between crosslinks l_c with the mesh size ξ, ignored the potential transition from the tight to loose bundle regime for the moment, and plotted G_0 as a function of single chain persistence length $l_{p,0}$ and N (Fig. 4). The plot highlights that even for intrinsically very stiff polymers bundling is a prerequisite for good mechanical properties of the gel, for instance a 1kPa gel (dotted line) can be prepared from very stiff single polymer chains as well as much more flexible, but bundled polymers. Controlling bundling presents a current challenge for molecular chemists, since it allows tuning the gel moldulus as well as the pore size $\approx l_c \propto N\sqrt[3]{c}$ of the gel. This analysis is completely in line with how Nature controls the mechanical properties of her cytoskeletal soft materials: taking stiff protein elements (a variety of

elements of different dimensions provide flexibility in the design) and controlling the amount of bundling by regulating the concentration of crosslinking proteins or divalent cations.

In summary, we presented a truly artificial intermediate filaments mimic with all its characteristic properties. The helical polyisocyanide backbone plays a crucial role in providing an intrinsically stiff backbone and controlling the bundling process. This class of materials, however, goes beyond mimicking IF biogels, since network characteristics and functionality can be readily introduced through small modifications in the chemical structure, for instance order-disorder transition temperatures can be changed by the length of the ethylene glycol length or the intrinsic backbone stiffness by the amino acid sequence[6]. Moreover, functional groups can be introduced at the periphery of the polymer (through azide-acetylene click chemistry), that allow for the incorporation of a wide variety of (bio-)molecules or cross-linkers in the polymer, mimicking more closely the natural environment of the cell.

References and Notes

1. Kamm, R. D. & Mofrad, M. R. K. in *Cytoskeletal Mechanics: models and measurements* (eds M. R. K. Mofrad & R. D. Kamm) Ch. 1, 1-17 (Cambridge University Press, 2006).
2. Lin, Y.-C. *et al.* Origins of Elasticity in Intermediate Filament Networks. *Phys. Rev. Lett.* **104**, 058101 (2010).
3. Fernandez, P., Pullarkat, P. A. & Ott, A. A master relation defines the nonlinear viscoelasticity of single fibroblasts. *Biophys. J.* **90**, 3796-3805 (2006).
4. Schwartz, E., Le Gac, S., Cornelissen, J. J. L. M., Nolte, R. J. M. & Rowan, A. E. Macromolecular multi-chromophoric scaffolding. *Chem. Soc. Rev.* **39**, 1576-1599 (2010).
5. Cornelissen, J. J. L. M. *et al.* β-helical polymers from isocyanopeptides. *Science* **293**, 676-680 (2001).
6. Van Buul, A. M. et al. Stiffness versus architecture of single helical polyisocyanopeptides, *submitted for publication.*
7. Keereweer, B. *et al.* in *Functional Supramolecular Architectures* Vol. 1 (eds P. Samori & F. Cacialli) Ch. 5, 135-152 (VCH, 2011).
8. Examples of oligo(ethylene glycol) functionalized polyisocyanides derived from arylisocyanides (ref. 9) and isocyanopeptides (ref. 10) have recently been reported but their thermo responsive properties in aqueous solution and more specifically there hydrogelation abilities were not addressed.
9. Hase, Y. *et al.* Unexpected thermally stable, cholesteric liquid-crystalline helical polyisocyanides with memory of macromolecular helicity. *Chem.-Asian J.* **2**, 755-763 (2007).
10. Kitto, H. J. *et al.* Post-modification of helical dipeptido polyisocyanides using the 'click' reaction. *J. Mater. Chem.* **18**, 5615-5624 (2008).
11. Tiller, J. C. Increasing the local concentration of drugs by hydrogel formation. *Angew. Chem.-Int. Ed.* **42**, 3072-3075 (2003).

12. Place, E. S., Evans, N. D. & Stevens, M. M. Complexity in biomaterials for tissue engineering. *Nat. Mater.* **8**, 457-470 (2009).

13. Peppas, N. A., Hilt, J. Z., Khademhosseini, A. & Langer, R. Hydrogels in biology and medicine: From molecular principles to bionanotechnology. *Adv. Mater.* **18**, 1345-1360 (2006).

14. Hirst, A. R., Escuder, B., Miravet, J. F. & Smith, D. K. High-Tech Applications of Self-Assembling Supramolecular Nanostructured Gel-Phase Materials: From Regenerative Medicine to Electronic Devices. *Angew. Chem.-Int. Ed.* **47**, 8002-8018 (2008).

15. Rowan, A. E. *et al.* Method for the preparation of high molecular weight oligo(alkylene glycol) functionalized polyisocyanopeptides Eur.Pat. EP 2287221 (2011).

16. Polymers **P2a** and **P3a** did not form gels, but precipitated forming a cloudy suspension, while **P1** failed did not dissolve in water. Its anticipated gel temperature is below 0 °C.

17. The absolute height found from the AFM images is constistantly too low. Typical values for an isolated chain of 0.5 nm are found. Considering that a diameter of the peptidic polymer (even without the glycol substituents) is already 2 nm, we are only able to use the relative height distributions to estimate the bundle numbers.

18. Grason, G. M. & Bruinsma, R. F. Chirality and equilibrium biopolymer bundles. *Phys. Rev. Lett.* **99** (2007).

19. Pollard, T. D. & Cooper, J. A. Actin and actin-binding proteins-a critical evaluation of mechanisms and functions. *Ann. Rev. Biochem.* **55**, 987-1035 (1986).

20. Leterrier, J. F., Kas, J., Hartwig, J., Vegners, R. & Janmey, P. A. Mechanical effects of neurofilament cross-bridges - Modulation by phosphorylation, lipids, and interactions with F-actin. *J. Bio. Chem.* **271**, 15687-15694 (1996).

21. Han, S., Hagiwara, M. & Ishizone, T. Synthesis of thermally sensitive water-soluble polymethacrylates by living anionic polymerizations of oligo(ethylene glycol) methyl ether methacrylates. *Macromolecules* **36**, 8312-8319 (2003).

22. Lutz, J. F. & Hoth, A. Preparation of ideal PEG analogues with a tunable thermosensitivity by controlled radical copolymerization of 2-(2-methoxyethoxy)ethyl methacrylate and oligo(ethylene glycol) methacrylate. *Macromolecules* **39**, 893-896 (2006).

23. Wang, H. *et al.* A structure-gelation ability study in a short peptide-based 'Super Hydrogelator' system. *Soft Matter* **7**, 3897-3905 (2011).

24. Mackintosh, F. C., Kas, J. & Janmey, P. A. Elasticity of semiflexible biopolymer networks. *Phys. Rev. Lett.* **75**, 4425-4428 (1995).

25. Gardel, M. L. *et al.* Elastic behavior of cross-linked and bundled actin networks. *Science* **304**, 1301-1305 (2004).

26. Mason, T. G., Dhople, A. & Wirtz, D. Linear viscoelastic moduli of concentrated DNA solutions. *Macromolecules* **31**, 3600-3603 (1998).

27. Storm, C., Pastore, J. J., MacKintosh, F. C., Lubensky, T. C. & Janmey, P. A. Nonlinear elasticity in biological gels. *Nature* **435**, 191-194 (2005).

28. Onck, P. R., Koeman, T., van Dillen, T. & van der Giessen, E. Alternative explanation of stiffening in cross-linked semiflexible networks. *Phys. Rev. Lett.* **95** (2005).

29. Huisman, E. M., van Dillen, T., Onck, P. R. & Van der Giessen, E. Three-dimensional cross-linked F-actin networks: Relation between network architecture and mechanical behavior. *Phys. Rev. Lett.* **99** (2007).

30. Broedersz, C. P. & MacKintosh, F. C. Molecular motors stiffen non-affine semiflexible polymer networks. *Soft Matter* **7**, 3186-3191 (2011).

31. Bustamante, C., Marko, J. F., Siggia, E. D. & Smith, S. Entropic elasticity of λ-phage DNA. *Science* **265**, 1599-1600 (1994).

32. For a quantitative description of the microstructure of the gel, rheological models based on reference 24 have been used. This model has been modified for the polyisocyanopeptides, for instance to correct for the unusual thermal behaviour and for the fact that bundling in this systems is independent of the concentration. The details of the model and the consequences are equated in the Supplementary Material.

33. Bathe, M., Heussinger, C., Claaessens, M. M. A. E., Bausch, A. R. & Frey, E. Cytoskeletal bundle mechanics. *Biophysical Journal* **94**, 2955-2964 (2008).

Acknowledgments

We thank Ben Norder for assistance with rheological experiments, Chase Broersz for support with the nonlinear rheology and Fred MacKintosh for fruitful discussion on interpretation of the semi-flexible polymer network theory. We acknowledge financial support from Technology Foundation STW, NanoNed, The Council for the Chemical Sciences of the Netherlands Organisation for Scientific Research, the Royal Academy for Arts and Sciences, NRSCC, and the EU projects Hierarchy (PITN-CT-2007-215851) and Superior (PITN-CT-2009-238177).

Author contribution

P.K. and A.R. wrote the manuscript and developed the model. M.K, T.W., E.S., H.K and R.H. were involved in the design, synthesis and characterization of the materials. M.J. and A.v.B. conducted the SMFS measurements. V.L.S., P.K., E.M. and S.P. designed, conducted and interpreted the rheological experiment, P.K., R.N. and A.R. supervised the project.

Supplementary Materials

Synthesis and characterization, CD measurements, AFM Analysis, Single Particle Tracking analysis, Vial inversion test, Rheology, Single Molecule Force Microscopy analysis, Semi-flexible network theory, References and Notes.